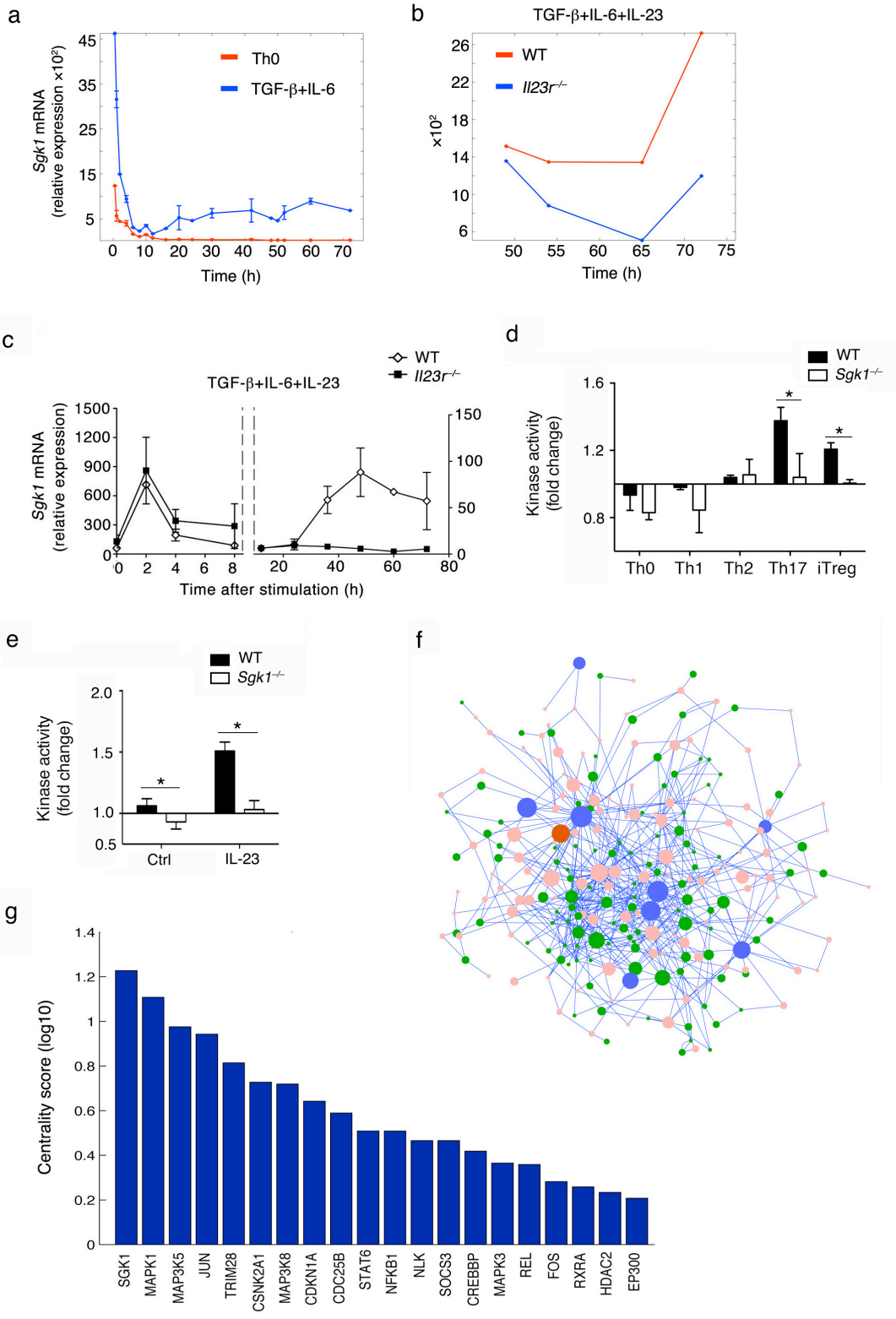
a
Sgk1 mRNA (relative expression ×10²)
Th0
TGF-β+IL-6
Time (h)
b
TGF-β+IL-6+IL-23
WT
Il23r−/−
×10²
Time (h)
c
TGF-β+IL-6+IL-23
WT
Il23r−/−
Sgk1 mRNA (relative expression)
Time after stimulation (h)
d
WT
Sgk1−/−
Kinase activity (fold change)
Th0
Th1
Th2
Th17
iTreg
e
WT
Sgk1−/−
Kinase activity (fold change)
Ctrl
IL-23
f
g
Centrality score (log10)
SGK1
MAPK1
MAP3K5
JUN
TRIM28
CSNK2A1
MAP3K8
CDKN1A
CDC25B
STAT6
NFKB1
NLK
SOCS3
CREBBP
MAPK3
REL
FOS
RXRA
HDAC2
EP300

Supplementary Fig. 1 SGK1 expression and activity in Th17 cells. (a) SGK1 expression level based on genome-wide mRNA analysis under Th0 and Th17 conditions at 18 different time points; (b) SGK1 expression based on genome-wide mRNA analysis in WT and *Il23r*$^{-/-}$ CD4^{+} T cells stimulated with TGF-β1, IL-6 and IL-23; (c) Kinetics of SGK1 gene expression in WT or *Il23r*$^{-/-}$ CD4^{+} T cells differentiated with TGF-β1, IL-6 and IL-23. mRNA expression data are presented relative to GAPDH expression; (d, e) SGK1 kinase activity in different T cell subsets and IL-23 restimulated Th17 cells. Data are representative of three independent experiments (error bars, SD); (f) IL-23R protein-protein interaction network model. Nodes are sized proportional to their network score. Network composed of all the protein nodes with a p-value under 10^{-4}; (g) Ranked list of nodes (proteins) sorted by their score in the IL-23R network model. **P*< 0.05 (Student's *t*-test).

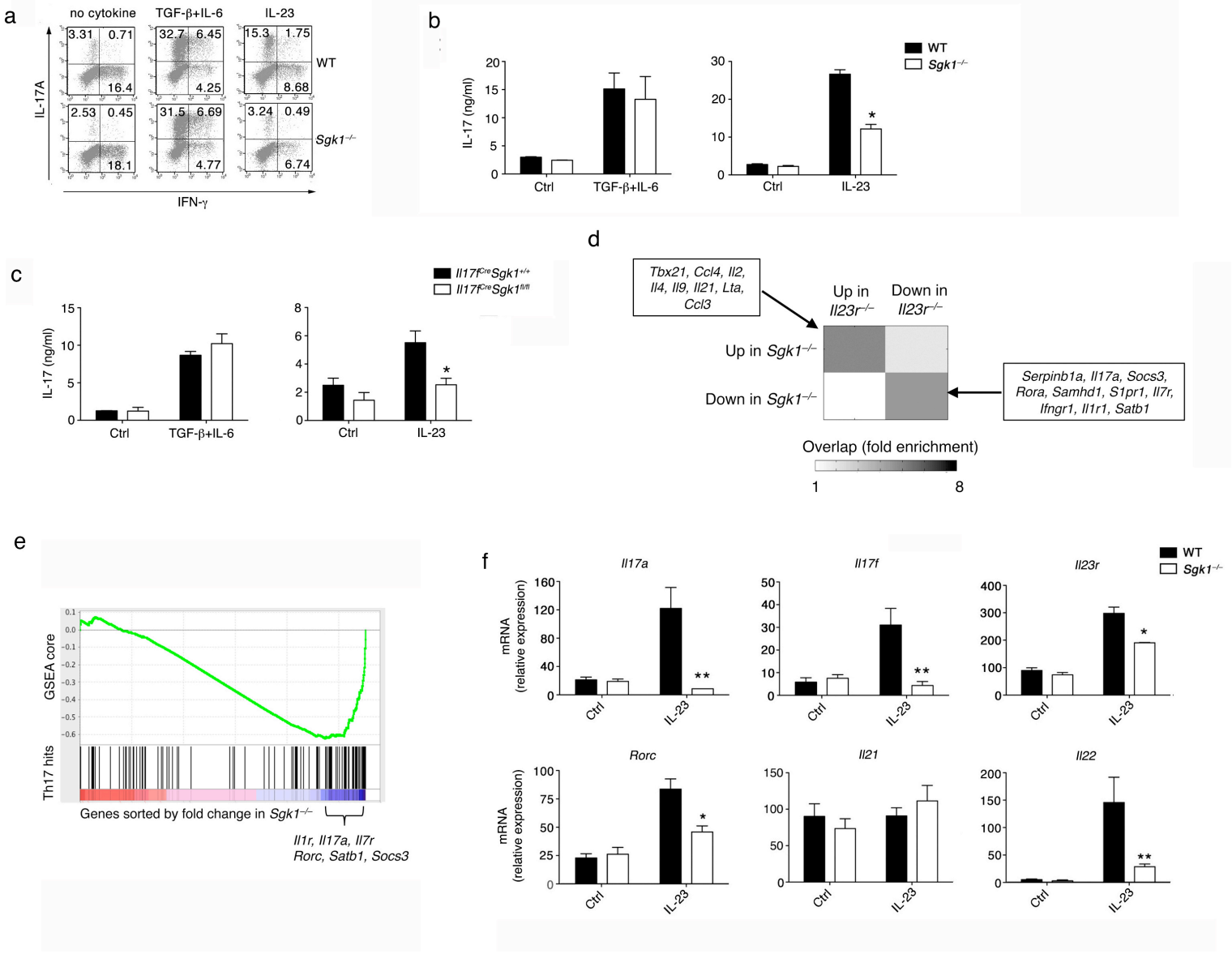

Supplementary Fig. 2 SGK1 deficiency impairs IL-23-dependent maintenance of Th17 cells *in vitro*. (a) IL-17A and IFN-γ production from WT and *Sgk1*$^{-/-}$ memory CD4^{+} T cells differentiated under indicated Th17 differentiation conditions; (b, c) IL-17 and IFN-γ production in the supernatants from cells described in Fig. 1e, f were measured by ELISA; (d) Overlap between the *Il23r*$^{-/-}$ and *Sgk1*$^{-/-}$microarray datasets**.** Differentially expressed genes in the *Il23r*$^{-/-}$ data are compared to the differentially expressed genes in

the *Sgk1*$^{-/-}$ data. Overlap is computed separately for the up- and down-regulated sets. Only significant results ($p<10^{-3}$) are presented. (e) Gene Set Enrichment Analysis (GSEA) of the *Sgk1*$^{-/-}$ microarray data showing that WT Th17-specific genes tend to be down-regulated in *Sgk1*$^{-/-}$ Th17 cells; (f) Differentiated WT and *Sgk1*$^{-/-}$ Th17 cells were restimulated with IL-23 and expression of indicated genes was analyzed by q-PCR analysis at 4 h after stimulation with PMA and ionomycin. **P*< 0.05 and ***P*< 0.01 (Student's *t*-test, error bars, SD). Data are representative of three independent experiments.

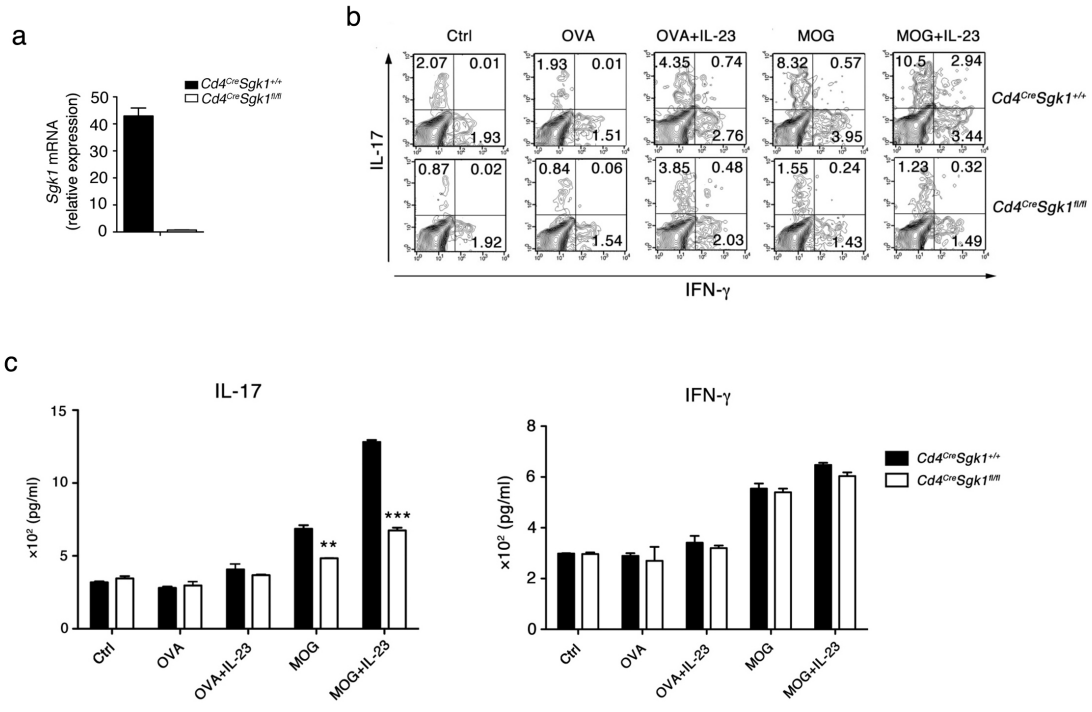

Supplementary Fig. 3 Impaired recall response of SGK1-deficient T cells. (a) mRNA level of SGK1 in *Cd4*^{Cre}*Sgk1*$^{+/+}$ and *Cd4*^{Cre}*Sgk1*$^{fl/fl}$ CD4^{+} T cells confirming lack of SGK1 expression in SGK1-deficient CD4^{+} T cells. Flow cytometry analysis (b) and ELISA (c) of IL-17 and IFN-γ production by CD4^{+} T cells isolated from immunized *Cd4*^{Cre}*Sgk1*$^{+/+}$ or *Cd4*^{Cre}*Sgk1*$^{fl/fl}$ mice and restimulated with the indicated antigens and IL-23 for 96 h. Data represents the means of two independent experiments. $^{**}P < 0.01$ and $^{***}P < 0.001$ (Student's *t*-test, error bars, SD).

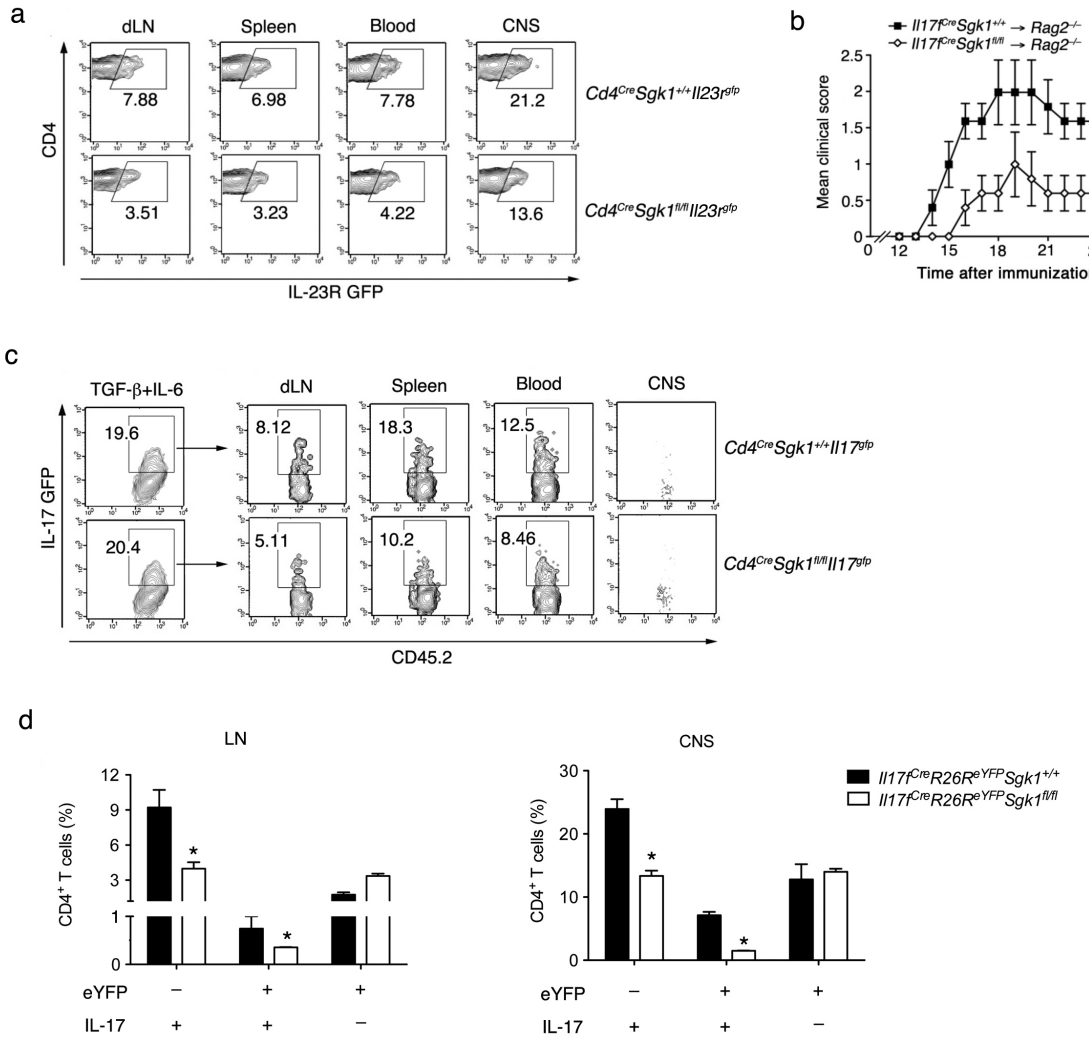

Supplementary Fig. 4 Impaired Th17 cell maintenance in the absence of SGK1 during EAE development. (a) IL-23R (GFP) expression on $CD4^+$ T cells isolated from the indicated organs of $Cd4^{Cre}Sgk1^{fl/fl}Il23r^{gfp}$ or control mice at the peak of EAE; (b) EAE disease course in $Rag2^{-/-}$ mice adoptively transferred with control or $Il17f^{Cre}Sgk1^{fl/fl}$ $CD4^+$ T cells (n=9); (c) IL-17 production from donor $CD4^+$ cells harvested from the indicated organs 7 days after transfer (n=9); (d) $CD4^+eYFP^+$ T cells isolated from LN and CNS of WT and SGK1-deficient $Il17f^{Cre}R26R^{eYFP}$ reporter mice 17 days after MOG-CFA

immunization, quantification of IL-17A production is shown as bar graph (n=10). Data are representative of three independent experiments. *$P < 0.05$ (Student's *t*-test).

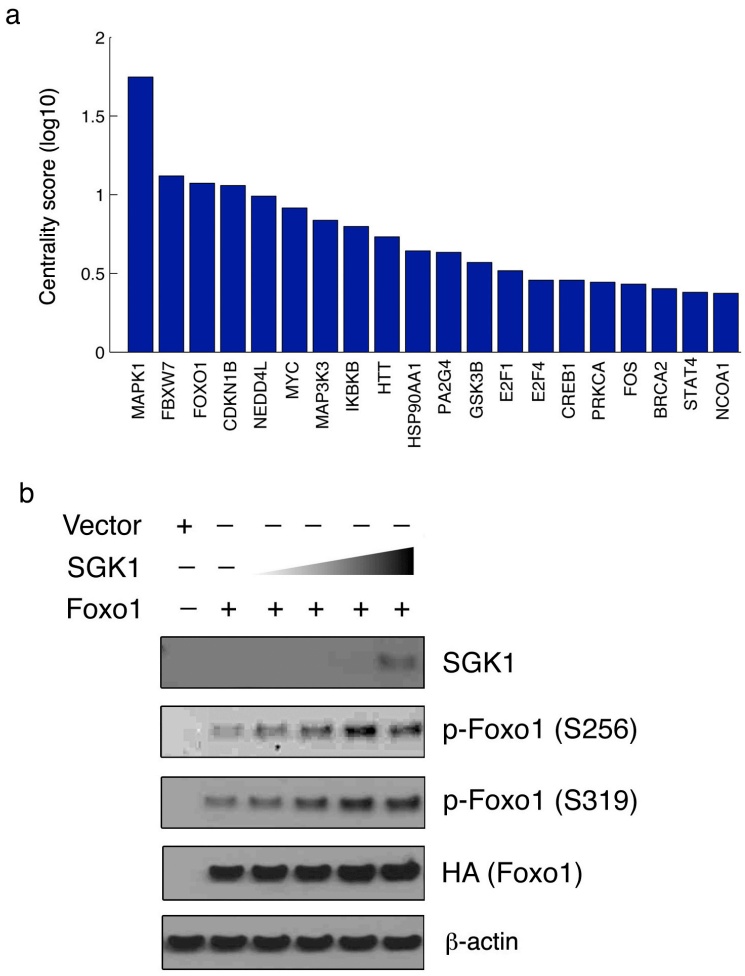

Supplementary Fig. 5 SGK1-Foxo1 signaling axis. (a) Ranked list of nodes (proteins) sorted by their score in the SGK1 network model (Methods); (b) To detect levels of Foxo1 phosphorylation, HEK293T cells were transfected with MSCV-IRES-GFP-SGK1 and pCMV5-Foxo1 (HA) constructs and lysates were prepared. The data shows that overexpression of SGK1 increases the levels of phosphorylated Foxo1 (S256 and S319). Data are representative of two independent experiments.

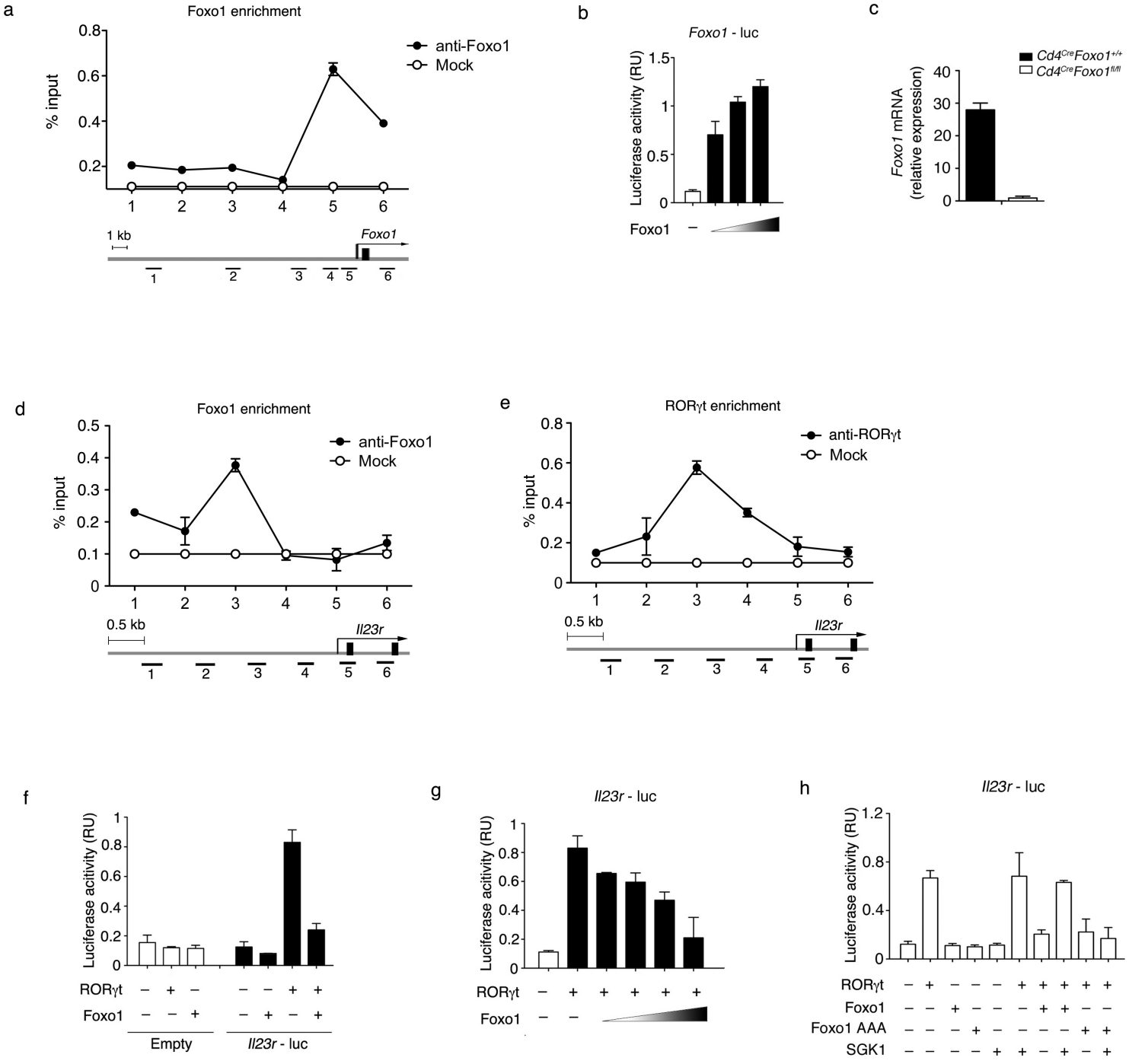
a
Foxo1 enrichment
anti-Foxo1
Mock
% input
1 kb
Foxo1
b
Foxo1 - luc
Luciferase acitivity (RU)
Foxo1
c
Cd4CreFoxo1+/+
Cd4CreFoxo1fl/fl
Foxo1 mRNA (relative expression)
d
Foxo1 enrichment
anti-Foxo1
Mock
% input
0.5 kb
Il23r
e
RORγt enrichment
anti-RORγt
Mock
% input
0.5 kb
Il23r
f
Luciferase acitivity (RU)
RORγt
Foxo1
Empty
Il23r - luc
g
Il23r - luc
Luciferase acitivity (RU)
RORγt
Foxo1
h
Il23r - luc
Luciferase acitivity (RU)
RORγt
Foxo1
Foxo1 AAA
SGK1

Supplementary Fig. 6 Foxo1 promotes its own expression and inhibits *Il23r* expression. (a) ChIP analysis of the interaction of Foxo1 or isotype control antibody with the *Foxo1* promoter regions in WT IL-23 restimulated Th17 cells; (b) HEK293T cells were transfected with a *Foxo1* promoter-driven luciferase reporter along with the indicated plasmids and promoter activity was determined; (c) mRNA level of Foxo1 in $Cd4^{Cre}Foxo1^{fl/fl}$ $CD4^+$ T cells; (d, e) ChIP analysis of the interaction of Foxo1 (d) or RORγt (e) or isotype control antibody with the *Il23r* promoter regions in WT IL-23 restimulated Th17 cells; (f-h) HEK293T cells were transfected with a *Il23r* promoter-driven luciferase reporter along with the indicated plasmids and promoter activity was determined. Data are representative of three independent experiments.

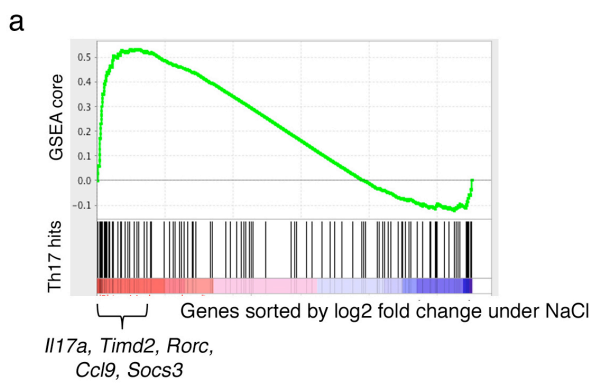
a
GSEA core
Th17 hits
Genes sorted by log2 fold change under NaCl
Il17a, Timd2, Rorc,
Ccl9, Socs3

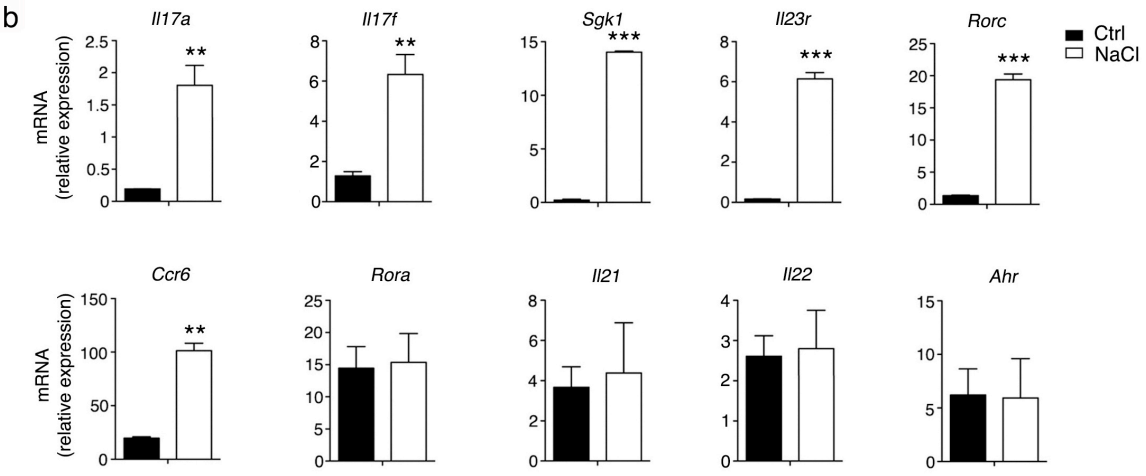
b
Il17a
Il17f
Sgk1
Il23r
Rorc
Ctrl
NaCl
mRNA
(relative expression)
Ccr6
Rora
Il21
Il22
Ahr

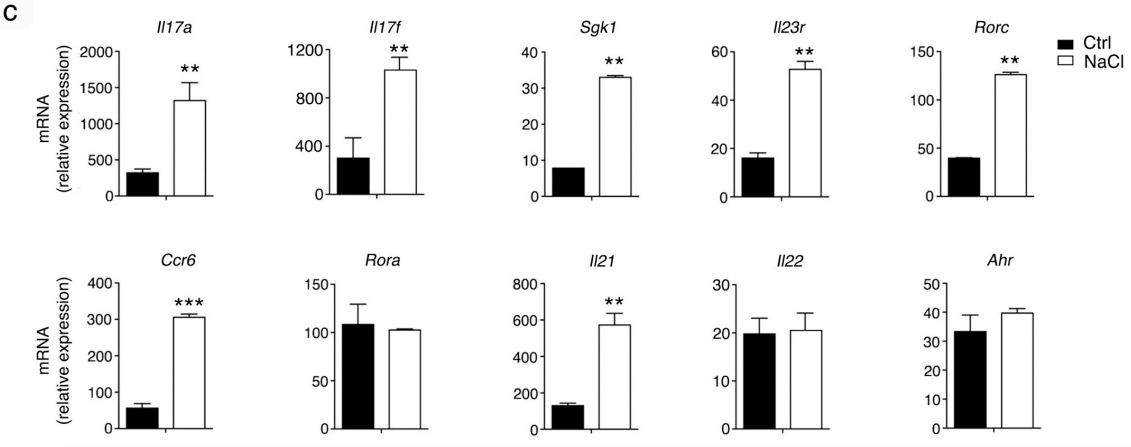
c
Il17a
Il17f
Sgk1
Il23r
Rorc
Ctrl
NaCl
mRNA
(relative expression)
Ccr6
Rora
Il21
Il22
Ahr

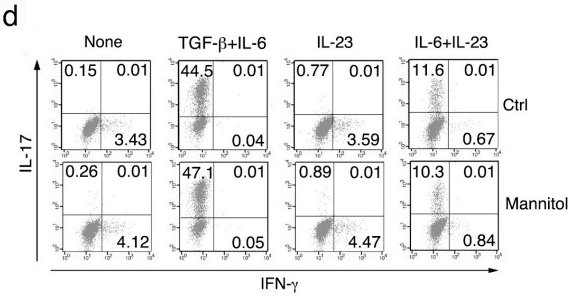
d
None
TGF-β+IL-6
IL-23
IL-6+IL-23
Ctrl
Mannitol
IL-17
IFN-γ
0.15
0.01
3.43
44.5
0.01
0.04
0.77
0.01
3.59
11.6
0.01
0.67
0.26
0.01
4.12
47.1
0.01
0.05
0.89
0.01
4.47
10.3
0.01
0.84

Supplementary Fig. 7 NaCl induces and enhances expression of Th17 cell signature genes. (a) Gene Set Enrichment Analysis (GSEA) of the NaCl microarray data showing that Th17-specific genes tend to be up-regulated in the presence of additional 40 mM NaCl; (b) mRNA expression of indicated genes in naïve WT $CD4^+$ T cells stimulated +/− 40 mM NaCl under Th0 conditions at 72 h; (c) mRNA expression of indicated genes in naïve WT $CD4^+$ T cells stimulated with 40 mM NaCl under Th17 differentiating conditions (TGF-β and IL-6) at 72 h; (d) IL-17 and IFN-γ production at 72 h in $CD4^+$ T cells differentiated in the presence of indicated cytokines +/− mannitol. $^{**}P< 0.01$ and $^{***}P< 0.001$ (Student's *t*-test, error bars, SD). Data are representative of three independent experiments.

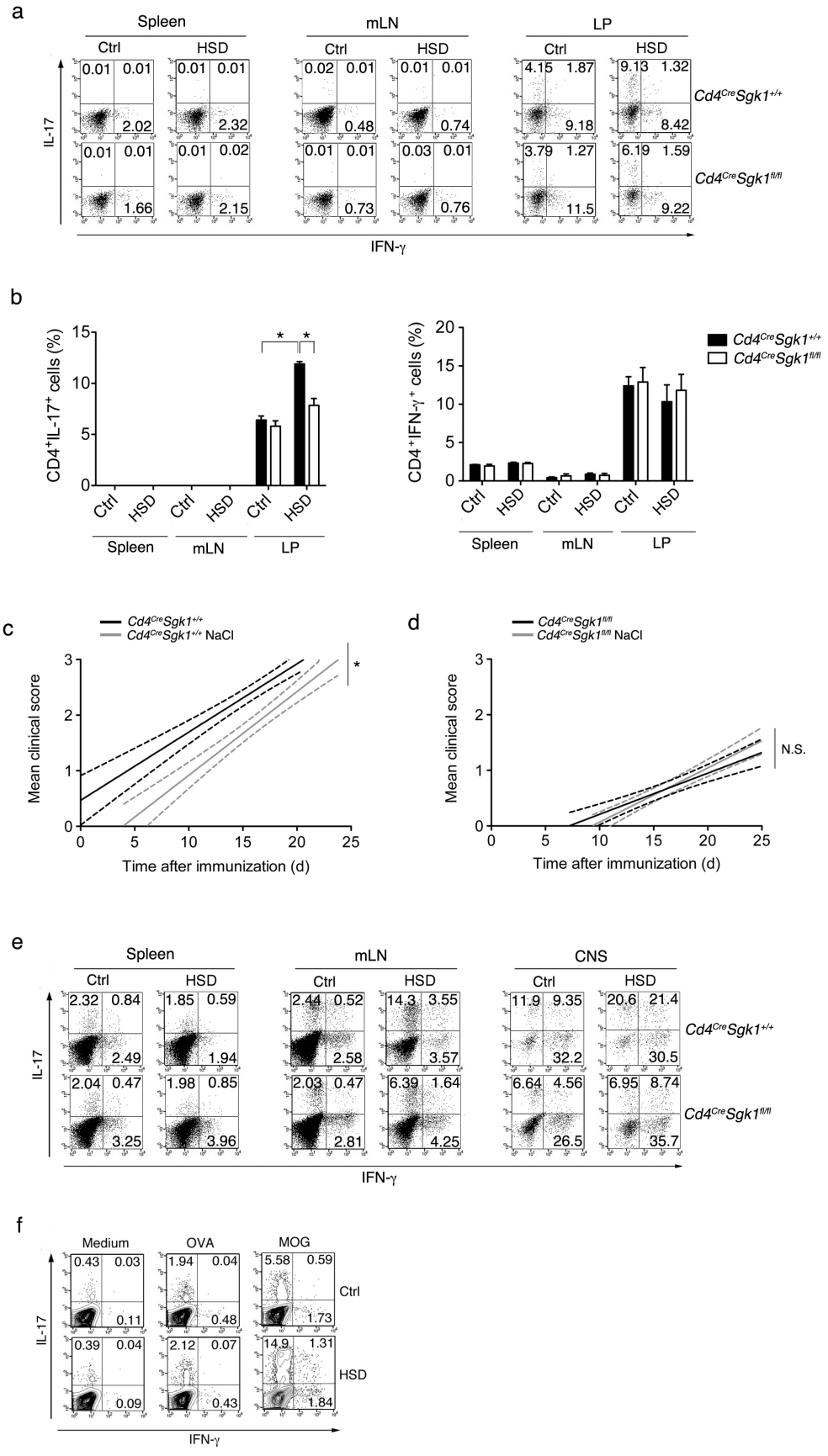
a
Spleen
mLN
LP
Ctrl
HSD
IL-17
IFN-γ
Cd4CreSgk1+/+
Cd4CreSgk1fl/fl
b
CD4+IL-17+ cells (%)
CD4+IFN-γ+ cells (%)
Spleen
mLN
LP
c
Cd4CreSgk1+/+
Cd4CreSgk1+/+ NaCl
Mean clinical score
Time after immunization (d)
d
Cd4CreSgk1fl/fl
Cd4CreSgk1fl/fl NaCl
N.S.
e
CNS
f
Medium
OVA
MOG

Supplementary Fig. 8 SGK1 is essential for high salt-induced autoimmunity. (a) Representative flow cytometry plots of $CD4^+IL\text{-}17^+$ or $CD4^+IFN\text{-}\gamma^+$ T cells from the indicated organs of $Cd4^{Cre}Sgk1^{+/+}$ and $Cd4^{Cre}Sgk1^{fl/fl}$ mice fed HSD or control diet for 3 weeks; (b) Quantification of $CD4^+IL\text{-}17^+$ or $CD4^+IFN\text{-}\gamma^+$ T cells from the indicated organs of naive WT mice fed HSD or control diet for 3 weeks; (c, d) Linear-regression curves of clinical scores of EAE in $Cd4^{Cre}Sgk1^{+/+}$ and $Cd4^{Cre}Sgk1^{fl/fl}$ mice fed with HSD or control diet as in Fig. 4e; (e) Representative flow cytometry plots of $CD4^+IL\text{-}17^+$ or $CD4^+IFN\text{-}\gamma^+$ T cells from the indicated organs of $Cd4^{Cre}Sgk1^{+/+}$ and $Cd4^{Cre}Sgk1^{fl/fl}$ mice fed HSD or control diet on day 17 following immunization with MOG/CFA; (f) Intracellular cytokine production of IL-17 and IFN-γ by $CD4^+$ T cells isolated from immunized WT mice fed HSD or control diet and re-stimulated with the indicated antigens for 96 h, as determined by flow cytometry. $^*P< 0.05$ (Student's *t*-test). Data are representative of three independent experiments (error bars, SD).

Supplementary Table. 1 Candidate selection in the *Il23r*$^{-/-}$ and *Sgk1*$^{-/-}$ data sets.

Sheet 1 (TF analysis – IL-23R): TF that are potentially dysregulated in *Il23r*$^{-/-}$ cells. The analysis is based on significance of overlaps (p-value, column 3) between their known target genes (data sources are listed in column 2) and the differentially expressed genes. **Sheet 2 (Ranking – IL-23R network)** – ranked list of candidate genes (top 20) in *Il23r*$^{-/-}$ cells. Top table – ranking based on expression profiles. Displayed data is fold change of expression. Bottom table – ranking based on network analysis. **Sheet 3 (TF analysis - SGK1):** TF that are potentially dysregulated in *Sgk1*$^{-/-}$ cells. The analysis is based on significance of overlaps (p-value, column 3) between their known target genes (data sources are listed in column 2) and the differentially expressed genes. **Sheet 4 (Ranking - SGK1 network):** ranked list of candidate genes (top 20) in *Sgk1*$^{-/-}$ cells based on network analysis.

Supplementary Table. 2 Microarray data analysis.

Sheet 1 (Differentially expressed genes): microarray-based expression fold changes (log2) in the *Il23r*$^{-/-}$ (vs. WT during the 65-72 h segment), *Sgk1*$^{-/-}$ (vs. WT) and NaCl (vs. no treatment) datasets. Only genes that are significantly differentially expressed in at least one condition are displayed. Value of "NA" in the *Il23r*$^{-/-}$ column indicates that the respective gene was not included in the array. **Sheet 2 (Functional enrichments)**: functional enrichment analysis based on the DAVID and MsgiDB databases. In the first column (gene set), "SGK1-up" corresponds to all genes that are up-regulated in the *Sgk1*$^{-/-}$Th17 cells; "SGK1-dn" corresponds to all genes that are down-regulated in the *Sgk1*$^{-/-}$ Th17 cells; "SGK1" corresponds to all genes that are differentially expressed (either up-

or downregulated) in *Sgk1*$^{-/-}$ cells. Similar annotation is used for the NaCl data.

Experimental Procedures

Animals

C57BL/6 (B6), CD45.1, *R26R*^{eYFP}, *Rag2*$^{-/-}$ mice were purchased from Jackson Laboratory; *Cd4*^{Cre} mice were purchased from Taconic; *Il17a*^{gfp} mice were purchased from Biocytogen; *Il23r*^{gfp}, *Il23r*$^{-/-}$, *Sgk1*$^{-/-}$, *Sgk1*$^{fl/fl}$, *Foxo1*$^{fl/fl}$ and *Il17f*^{Cre} mice have been described previously [1, 2, 3, 4]. All experiments were carried out in accordance with guidelines prescribed by the Institutional Animal Care and Use Committee (IACUC) at Harvard Medical School.

Antibodies

The following antibodies were used in flow cytometry and cell sorting: CD45.2 (104, eBiosciences), CD4 (H129.19, BD Pharmingen), IL-17A (TC11-18H10.1, BD Pharmingen), IL-17F (9D3.1C8, Biolegend), IFN-γ (XMG1.2, BD Pharmingen), CD44 (IM7, Biolegend), CD62L (MEL-14, Biolegend).

Active EAE

EAE was induced using the 35–55 peptide of myelin/oligodendrocyte glycoprotein (MOG_{35-55}) as previously described [5].

In vitro T cell differentiation

Sorted naïve $CD4^+$ T cells ($CD4^+CD62L^+CD44^-$) were activated with plate-bound anti-CD3 (2 ug/ml; 145-2C11) and anti-CD28 (2 ug/ml; PV-1). The naive cells were cultured at a concentration of 2×10^6 /ml in IMDM medium supplemented with 10% FBS, L-

glutamine, HEPES, penicillin/streptomycin, gentamicin sulfate, and 2-ME. For the generation of Th17 cells, naive T cells (1×10^6/ml) were cultured with IL-6 (30 ng/ml) and TGF-β1 (3 ng/ml) on 24 well plates for 72 h. The differentiated Th17 cells (1×10^6/ml) were then transferred into blank 24 well plates in the fresh medium to rest for 72 h, following with IL-23 (20 ng/ml) restimulation in the presence of anti-CD3/28 for 72 h. IL-12 (10 ng/ml) and anti-IL-4 (10 μg/ml; 11B11) for Th1 differentiation; or IL-4 (10 ng/ml) and anti-IL-12 (10 μg/ml) for Th2 differentiation; or TGF-β1 (5 ng/ml) for Treg differentiation; IL-1β (10 ng/ml), IL-21 (50 ng/ml) for Th17 differentiation. Mouse IL-6, TGF-β1, IL-23, IL-4 and IL-12 were purchased from Miltenyi. IL-1β and IL-21 were purchased from (R&D system).

Flow cytometry

Mice were perfused with PBS before spleens, LNs and brains were harvested. Spleens and brains were pretreated with 2 μg/ml collagenase D and 1 μg/ml DNAse I (both Roche Diagnostics), and total cells were isolated by cell straining (70 μm for spleens/ 100 μm for brains). Brain homogenates were separated into neuronal and leukocyte populations by discontinuous density gradient centrifugation using isotonic Percoll (Amersham). Cells were permeablized and fixed with an intracellular staining kit (eBioscience); Annexin V/PI staining was carried out following the manufacturer's instructions (BD Biosciences). Flow cytometry was performed using a FACS Calibur (Becton Dickinson) with the antibodies listed above.

Quantitative RT-PCR

Cells were stimulated as indicated and RNA was extracted using RNeasy minikits (Qiagen). RNA expression was detected by RT-PCR with the GeneAmp 7500 Sequence Detection System or the ViiA7 Real-Time PCR System (Applied Biosystems). Expression levels were normalized to the expression of GAPDH. Primer-probe mixtures were purchased from Applied Biosystems. *Ahr* (Mm00478932-m1); *Ccr6* (Mm99999114-s1); *Foxo1* (Mm00490672-m1); *Il17a* (Mm00439619-m1); *Il17f* (Mm00521423-m1); *Il21* (Mm00517640-m1); *Il22* (Mm01226722-g1); *Il23r* (Mm00519943-m1); *Rora* (Mm01173766-m1); *Rorc* (Mm01261022-m1); *Sgk1* (Mm00441380-m1); *GAPDH* (4352339E)

Cytokine production

Sorted naïve $CD4^+$ T cells were stimulated as indicated. Cytokine concentration was determined by ELISA as previously published [6].

Western blot analysis

2-5 x 10^6 cells were lysed in whole cell extract buffer (50 mM Tris-HCl, pH 7.5, 150 mM NaCl, 0.5% Igepal CA-630, 0.2 mM EDTA, 10 mM Na2VO4, 10% glycerol, protease inhibitors) to obtain whole cell lysates. Alternatively, nuclear lysates were prepared with a nuclear extract kit following the manufacturer's instructions (Active Motif). Proteins were separated by SDS-PAGE gel electrophoresis using 4-12% NuPAGE Bis-Tris gels (Invitrogen) followed by transfer to nitrocellulose membrane. To block unspecific binding, membranes were incubated with 5% milk in TBST (0.5 M NaCl, Tris-HCl, pH 7.5, 0.1% (v/v) Tween-20) for 60 min and washed once with TBST. Proteins of interest

were detected by incubating membranes over night at 4°C in 5% BSA/TBST with the indicated antibodies (listed below), washing with TBST three times 10 min and incubating with horseradish peroxidase–conjugated anti-rabbit or anti-mouse antibody (Cell Signaling, 7074 and 7076). Bound antibody was detected by using Immobilon Western chemiluminescent HRP substrate (Millipore). Antibodies used for Western blot analysis: anti-Foxo1 (Cell Signaling, 2880), anti-p-Foxo1 (S256) (Cell Signaling, 9461), anti-p-Foxo1 (S319) (Santa Cruz, sc-23771R), anti-SGK (Cell Signaling, 3272), anti-HA tag (C29F4, Cell Signaling), anti-β-Actin (Santa Cruz, sc-47778), anti-β-Tubulin (AA2, Millipore), anti-Histone H3 (3H1, Cell Signaling).

Immunoprecipitation

Cell lysates were prepared as described above and proteins were immunoprecipitated by incubation of lysates with 3 μg antibody (listed below) over night at 4°C and pull-down of antibody-protein precipitates with Dynabeads Protein G (Invitrogen). Beads were washed extensively and proteins eluted with NuPAGE LDS sample buffer (10% β-mercaptoethanol). The presence of immuncomplexed proteins was determined by Western blot analysis with the antibodies listed. Rabbit polyclonal anti-Foxo1 (ab39670, Abcam), mouse monoclonal anti-Foxo1 (C-9, Santa Cruz), rat monoclonal anti-RORγt (B2D, eBioscience), rabbit polyclonal anti-RORγt (H-190, Santa Cruz).

Kinase activity assay

Sorted naïve WT T cells were differentiated *in vitro*, as described above. Different T cell subsets were analysed 3 days after stimulation, whereas restimulated Th17 cells were

differentiated towards Th17 cells for 3 days, rested for 3 days and analysed after restimulation with IL-23 for 1 h. Cell lysates were prepared as described above and SGK1 was immunoprecipitated from the lysates with anti-SGK1 (Abcam, ab43606). The immunoprecipitate was washed extensively and SGK1 kinase activity was assessed with a luminescence-based assay (SGK1 kinase ADP-Glo™ Kinase Assay, Promega).

Plasmids

Murine SGK1 was cloned from pCMV-Sport6 (Openbiosystems, MMM1013-64329) into the MSCV-IRES-GFP vector at EcoRI and XhoI sites.

Reporter assays

HEK 293T cells (4 x 10^4 cells/well, 48 well plate) were transiently transfected with the indicated expression vectors, empty vector controls as well as the promoter Firefly luciferase-reporter constructs and Renilla luciferase reporter vector (Promega) with Fugene HD (Roche). 48 h after transfection, luciferase expression was determined by measuring luminescence with the Dual-Luciferase Reporter Assay System (Promega). The Firefly luciferase activity was normalized to Renilla luciferase activity. Data is representative of at least two independent experiments; each data point represents duplicate values. The following vectors were used; MSCV-IRES-GFP-SGK1, MSCV-IRES-GFP-RORγt (kind gift of Dr. Liang Zhou), pCMV5-Foxo1 (kind gift of Domenico Accili, Addgene, plasmid 12142), pCMV5-Foxo1AAA (kind gift of Domenico Accili, Addgene, plasmid 17547) pGL3-Foxo1 reporter (kind gift of Dr. Jean-Baptiste Demoulin), pTA-Luc IL23R reporter (kind gift of Dr. Kojiro Sato),

ChIP PCR

Naïve T cells were treated with the indicated cytokines. ChIP was performed according to manufacturer's instructions (Cell Signaling) and samples were analyzed by SYBR Green real-time PCR (primers described below). The following antibodies were used for ChIP: anti-Foxo1 (Abcam, ab39670), anti-RORγt (eBioscience, AFKJS-9).

Microarray data

Naïve T cells were isolated from WT and *Il23r*$^{-/-}$ mice, and were treated with IL-6, TGF-β1 and IL-23. Affymetrix microarray HT_MG-430A was used to measure the resulting mRNA levels at four different time points (49 h, 54 h, 65 h, 72 h).

As an additional dataset for generating the candidate list in Figure 1a we used gene expression profiles from WT naïve T cells treated with IL-6 and TGF-β1 (the generation of the list is explained in detail below). This data was collected from 18 time points (30 min to 72 h) using the Affymetrix microarray HT_MG-430A. As control, we used WT Th0 cells harvested at the same time points.

Th17 cells from WT and *Sgk1*$^{-/-}$ mice were restimulated with IL-23. Affymetrix microarray Mouse430_2 was used to measure the resulting mRNA levels in duplicate. For the analysis of the NaCl effect, naïve T cells were isolated from WT mice, and placed under Th0 conditions with or without 40 mM NaCl for 72 h. The resulting mRNA levels were then measured in duplicate with Affymetrix microarray Mouse430_2.

Expression data was preprocessed using the RMA algorithm followed by quantile normalization, using the default parameters in the ExpressionFileCreator module of the GenePattern suite [7].

Detection of differentially expressed genes

Genes that are differentially expressed in the *Il23r*$^{-/-}$ time course (compared to the WT time course) were found using three methods: **(1)** Fold change, reporting all genes that had more than 2-fold change (up or down) compared to the control sample during at least two time points. **(2)** Polynomial fit. We used the EDGE software [8], which was designed for identifying differential expression in time course data. We set a threshold of q-value <=0.01. **(3)** Sigmoidal fit. Using an algorithm similar to [8]. However, instead of polynomials we used a sigmoid function [9], which were recently observed as more adequate for modeling time course gene expression data. As above, we set a threshold of q-value <=0.01.

We defined all genes that pass at least two out of the three tests as differentially expressed. The reported fold change levels in Fig. 1h and Table S2 are the average over the last two time points (65 h, 72 h). To avoid spurious fold levels due to low expression values a small constant was added to the expression values (c=50). Collapsing of probesets into genes is done in the following way: for differentially expressed genes the average over all differentially expressed probesets was used. For other genes we used the probeset with the highest absolute expression level.

To find genes that are differentially expressed in the NaCl conditions or in *Sgk1*$^{-/-}$ cells (compared to the respective control) we computed fold changes between the expression levels of each probeset in the case and control conditions. To avoid spurious fold levels due to low expression values we added a small constant to the expression values as above. We only reported cases where more than 50% of the four possible case-control comparisons were over a cutoff of 1.5 fold change. As an additional filter, we computed a Z-score by comparing the mean of the expression levels in the case samples to the control samples. We only reported cases with a corresponding p-value lower than 0.05. We collapsed probesets into genes as above.

Overlap between the *Il23r*$^{-/-}$ and *Sgk1*$^{-/-}$ microarray datasets

We used the Fisher exact test to compare the list of differentially expressed genes in the *Il23r*$^{-/-}$ data and the differentially expressed genes in the *Sgk1*$^{-/-}$ data. Overlap was computed separately for the up- and down-regulated sets (4 combinations altogether; see Supplementary Fig. 2d).

Generating the candidate list for the *Il23r*$^{-/-}$ data

We ranked the genes based on the average of: **(1)** Average fold increase during the time segment (48-72 h), comparing WT naïve T cells treated with IL-6 and TGF-β1 to Th0 cells. **(2)** Average fold decrease during the time segment (65-72 h), comparing *Il23r*$^{-/-}$ and WT cells treated with IL-6, TGF-β1, and IL-23.

Network analysis of the *Il23r*$^{-/-}$ T cell data

We collected protein-protein interaction (PPI) data from several public databases ([10, 11, 12, 13], http://www.netpath.org/, and http://www.phosphosite.org/). Interactions from [10, 12, 13] are assigned with a confidence value in the range of [0…1], according to the experimental evidence that supports them as in [14]. Interactions from the SPIKE database [11] are assigned with a score using the confidence classification provided in the database. Specifically, the four confidence classes (from high to low) were associated with the confidence levels at the 10-th, 6-th, 3-rd, and 1-st quantile. Interactions from the curated databases PhosphoSite and NetPath were assigned a maximal confidence score of 1. Since most interactions are in humans, we used orthology mapping to transfer the interaction data to mice.

Based on manual literature curation, we collected a set of genes that are known to play a role in IL-23R signaling (termed the "IL-23R signaling set"). Those include: *Il23r, Il12rb1, Tyk2, Jak2, Akt1, Pik3r1, Pdk1, Stat3, Stat4*, and *Nfkbib*. We then used an in-house command line version of the ANAT software [14] for finding a PPI network that connects the IL-23R signaling set to the set of transcription factors (TF) whose activity is dysregulated under *Il23r*$^{-/-}$ (see next section for the identification of these responsive TF).

We considered several variations on the default application of ANAT: **(1)** Using only post-translational modifications (instead of all the PPI data available). **(2)** Penalizing high degree nodes (thus avoiding unspecific, and potentially irrelevant hub nodes). Here, we

set the curvature parameter to be 2 (i.e. the penalty is proportional to the square root of the degree). The dominance parameter is set such that the average node weight is equal to the average edge weight. **(3)** Introducing a bias, preferring genes that are differentially expressed in *Il23r*$^{-/-}$ cells. Here we assigned a prior confidence value of 1 to the differentially expressed genes, and a value of 0.5 to the remaining genes.

For a robust analysis, we applied ANAT using all eight possible "yes/no" combinations of these three variations. Each node in each of the eight resulting networks is associated with a p-value, denoting the probability for it to be included in the network by chance. For a given network and for each node with a p-value lower than 10^{-4}, we computed a centrality score (as in [14]) defined as the number of downstream TF whose path to the IL-23R signaling set passes through that node. Nodes that are not included in the network or have a p-value above the cutoff are associated with a centrality score of zero. We then reported the average score over all eight network configurations.

Network analysis of the *Sgk1*$^{-/-}$ T cell data

We utilized a similar analysis as above. ANAT was applied for finding a PPI network that connects SGK1 to the set of TF whose activity is dysregulated in *Sgk1*$^{-/-}$ cells (see next section for the identification of these responsive TF). As above, we computed eight different configurations. For the third variation (introduction of node bias) we used the genes that are differentially expressed in *Sgk1*$^{-/-}$ cells.

Identification of responsive TF in the *Sgk1*$^{-/-}$ T cell data

We identified TF that are potentially dysregulated in *Sgk1*$^{-/-}$ cells by looking for significant overlaps between their known target genes and the differentially expressed genes. TF-target interaction data was obtained from public databases [15, 16, 17, 18, 19, 20]. Additional potential interactions, were obtained by applying the SPC clustering algorithm [21] to data from the mouse ImmGen consortium (http://www.immgen.org; January 2010 release; [22]), which includes 484 microarray samples from 159 cell subsets from the innate and adaptive immune system of the mouse. For every TF in our database we computed the statistical significance of its overlap with the set of differentially expressed genes using the Fisher exact test. We reported cases with $p< 5\times10^{-5}$ and fold enrichment > 1.5.

We used two additional sources for the TF analysis: **(1)** a statistical analysis of binding-site enrichment in promoter regions that are associated with the differentially expressed genes using the PRIMA algorithm [23]. **(2)** The TF enrichment module of the commercial IPA software (http://www.ingenuity.com/). As above, we used a cutoff of $p <5\times10^{-5}$.

Identification of responsive TF in the *Il23r*$^{-/-}$ T cell data

The analysis of the *Il23r*$^{-/-}$ T cell data uses a similar strategy as the one applied to the *Sgk1*$^{-/-}$ T cell data. However, instead of only crossing the TF databases with the entire set of differentially expressed genes, we also used smaller clusters of genes that have similar temporal expression characteristics. We considered several ways for grouping the differentially expressed genes, based on their time course expression data: **(1)** For each time point, group all the genes that are over- or under-expressed during that time. **(2)** For each time point, group all the genes that showed a significant change in their expression

(increase/ decrease) as compared with the previous time point. **(3)** Cluster the genes based on their profiles under the knockout condition. We use k-means clustering with the minimal k such that the within cluster similarity (average pearson correlation with centroid) is higher than 0.75 for all clusters. **(4)** Cluster the genes based on a concatenation of their knockout profile and their WT profile (using k-means as before).

T cell subset signature genes

We downloaded and analyzed the gene expression data from [24] and pre-processed it using the RMA algorithm followed by quantile normalization, using the default parameters in the ExpressionFileCreator module of the GenePattern suite [7]. This data includes duplicate microarray measurements from Th17, Th1, Th2, iTreg, nTreg, and naïve $CD4^+$ T cells. For a given cell subset we evaluated for each gene whether it is over-expressed compared to all other cell subsets using a one-sided t-test. We retained all cases that had a p-value under 0.05. As an additional filtering step, we required that that the expression level of the gene in the given cell subset is at least 1.25 fold higher than its expression in all other cell subsets. As before, to avoid spurious fold levels due to low expression values we added a small constant to the expression values (c=50). We evaluated the overlap between differentially expressed genes (in either *Sgk1*$^{-/-}$ or NaCl-treated cells) and the subset-specific genes using Fisher exact test. As an additional test, we performed GSEA analysis [19] testing the correlation between the different T cell subsets and the fold change of genes in either *Sgk1*$^{-/-}$ or NaCl-treated cells. In this analysis, for a given T-cell subset, the "gene set" is the list of genes that are up-regulated in the subset; and the expression data set is the log-expression fold change.

Functional enrichment analysis

We used two sources for the functional enrichment test for the genes that are differentially expressed in either *Sgk1*$^{-/-}$ or NaCl-treated cells: **(1)** The DAVID functional annotation tool [25]; **(2)** The MsigDB database [19], using the "canonical pathway" subset of the curated gene set (c2.cp.v3.0), the "cellular process" subset of the Gene ontology gene set (c5.all.v3.0), and the motif gene set (c3.all.v3.0). We evaluate the significance of the MsigDB overlaps using the Fisher exact test.

Statistical analysis

Statistical analysis was performed using GraphPad Prism (GraphPad Software Inc., La Jolla, CA). The data were analyzed by a paired sign *t*-test or Student's *t*-test. All *P* values of 0.05 or less were considered statistically significant.

Sequences of primers used in chromatin immunoprecipitation (ChIP) assay

Foxo1 promoter 1 s	GAGTCAGGATCCCCAGACAA
Foxo1 promoter 1 as	AGACAGAAGAGGGCAGCAGA
Foxo1 promoter 2 s	GGCCAATGCTCTGCTACAAT
Foxo1 promoter 2 as	CCTGCAAGTTCAGGTGAGGT
Foxo1 promoter 3 s	TGTATCCCCTGCATCCTCA
Foxo1 promoter 3 as	TGGCAATGTTCTATTTCCTAAGGT
Foxo1 promoter 4 s	TTCACAGCTGGATTTCATCG
Foxo1 promoter 4 as	ATGGATGAGCCTAAGCAGGA
Foxo1 promoter 5 s	CGGTTTGCCTCCTAGCAAT
Foxo1 promoter 5 as	AGGCGGCAGTAGGTTGGT
Foxo1 promoter 6 s	ATGTATTAAATTGTTTTTCTCCTTGG
Foxo1 promoter 6 as	TGTCAAGCATCTATCTACTCCTCTG
Il23r promoter 1 s	AAGTTGGAGGCAGGGACATCAAGA
Il23r promoter 1 as	TGCTTGGCTTCTAGTTGGTGGACT
Il23r promoter 2 s	AGCCAGTACAGGAACCACAAGGAA
Il23r promoter 2 as	ACAAATGCCAAGAGGAGACAGGGA
Il23r promoter 3 s	TAGGGTTGGGAAATGAGGCTGACA
Il23r promoter 3 as	AAGGAGTGCAAGAGGAGCATTGGA
Il23r promoter 4 s	TGAAGCTTGGACACCAAGAGTCCT
Il23r promoter 4 as	TCTAGGCCAGGTGGTGGTTTGAAT
Il23r promoter 5 s	TCTCTCGTACTGCCAATTGCACCT
Il23r promoter 5 as	AGGCAGCACAAGCTGTAGAATTGC
Il23r promoter 6 s	AGAGTAGCTGCCTGATGAAGGACA
Il23r promoter 6 as	TTGAGCAGAGCATCAGGGTGGAAT

References:

1. Ouyang W, Beckett O, Ma Q, Paik JH, DePinho RA, Li MO. Foxo proteins cooperatively control the differentiation of Foxp3+ regulatory T cells. *Nature immunology* 2010, **11**(7)**:** 618-627.

2. Petermann F, Rothhammer V, Claussen MC, Haas JD, Blanco LR, Heink S*, et al.* gammadelta T cells enhance autoimmunity by restraining regulatory T cell responses via an interleukin-23-dependent mechanism. *Immunity* 2010, **33**(3)**:** 351-363.

3. Croxford AL, Kurschus FC, Waisman A. Cutting edge: an IL-17F-CreEYFP reporter mouse allows fate mapping of Th17 cells. *J Immunol* 2009, **182**(3)**:** 1237-1241.

4. Fejes-Toth G, Frindt G, Naray-Fejes-Toth A, Palmer LG. Epithelial Na+ channel activation and processing in mice lacking SGK1. *Am J Physiol Renal Physiol* 2008, **294**(6)**:** F1298-1305.

5. Stromnes IM, Goverman JM. Active induction of experimental allergic encephalomyelitis. *Nat Protoc* 2006, **1**(4)**:** 1810-1819.

6. Jager A, Dardalhon V, Sobel RA, Bettelli E, Kuchroo VK. Th1, Th17, and Th9 effector cells induce experimental autoimmune encephalomyelitis with different pathological phenotypes. *J Immunol* 2009, **183**(11)**:** 7169-7177.

7. Reich M, Liefeld T, Gould J, Lerner J, Tamayo P, Mesirov JP. GenePattern 2.0. *Nat Genet* 2006, **38**(5)**:** 500-501.

8. Storey JD, Xiao W, Leek JT, Tompkins RG, Davis RW. Significance analysis of time course microarray experiments. *Proceedings of the National Academy of Sciences of the United States of America* 2005, **102**(36)**:** 12837-12842.

9. Chechik G, Koller D. Timing of gene expression responses to environmental changes. *J Comput Biol* 2009, **16**(2)**:** 279-290.

10. Breitkreutz BJ, Stark C, Reguly T, Boucher L, Breitkreutz A, Livstone M*, et al.* The BioGRID Interaction Database: 2008 update. *Nucleic Acids Res* 2008, **36**(Database issue)**:** D637-640.

11. Elkon R, Vesterman R, Amit N, Ulitsky I, Zohar I, Weisz M*, et al.* SPIKE--a database, visualization and analysis tool of cellular signaling pathways. *BMC Bioinformatics* 2008, **9:** 110.

12. Peri S, Navarro JD, Amanchy R, Kristiansen TZ, Jonnalagadda CK, Surendranath V*, et al.* Development of human protein reference database as an initial platform for approaching systems biology in humans. *Genome Res* 2003, **13**(10)**:** 2363-2371.

13. Xenarios I, Salwinski L, Duan XJ, Higney P, Kim SM, Eisenberg D. DIP, the Database of Interacting Proteins: a research tool for studying cellular networks of protein interactions. *Nucleic Acids Res* 2002, **30**(1)**:** 303-305.

14. Yosef N, Zalckvar E, Rubinstein AD, Homilius M, Atias N, Vardi L*, et al.* ANAT: a tool for constructing and analyzing functional protein networks. *Sci Signal* 2011, **4**(196)**:** pl1.

15. Linhart C, Halperin Y, Shamir R. Transcription factor and microRNA motif discovery: the Amadeus platform and a compendium of metazoan target sets. *Genome Res* 2008, **18**(7)**:** 1180-1189.

16. Zheng G, Tu K, Yang Q, Xiong Y, Wei C, Xie L*, et al.* ITFP: an integrated platform of mammalian transcription factors. *Bioinformatics* 2008, **24**(20)**:** 2416-2417.

17. Wilson NK, Foster SD, Wang X, Knezevic K, Schutte J, Kaimakis P*, et al.* Combinatorial transcriptional control in blood stem/progenitor cells: genome-wide analysis of ten major transcriptional regulators. *Cell Stem Cell* 2010, **7**(4)**:** 532-544.

18. Lachmann A, Xu H, Krishnan J, Berger SI, Mazloom AR, Ma'ayan A. ChEA: transcription factor regulation inferred from integrating genome-wide ChIP-X experiments. *Bioinformatics* 2010, **26**(19)**:** 2438-2444.

19. Liberzon A, Subramanian A, Pinchback R, Thorvaldsdottir H, Tamayo P, Mesirov JP. Molecular signatures database (MSigDB) 3.0. *Bioinformatics* 2011, **27**(12)**:** 1739-1740.

20. Jiang C, Xuan Z, Zhao F, Zhang MQ. TRED: a transcriptional regulatory element database, new entries and other development. *Nucleic Acids Res* 2007, **35**(Database issue)**:** D137-140.

21. Blatt M, Wiseman S, Domany E. Superparamagnetic clustering of data. *Phys Rev Lett* 1996, **76**(18)**:** 3251-3254.

22. Heng TS, Painter MW. The Immunological Genome Project: networks of gene expression in immune cells. *Nature immunology* 2008, **9**(10)**:** 1091-1094.

23. Elkon R, Linhart C, Sharan R, Shamir R, Shiloh Y. Genome-wide in silico identification of transcriptional regulators controlling the cell cycle in human cells. *Genome Res* 2003, **13**(5)**:** 773-780.

24. Wei G, Wei L, Zhu J, Zang C, Hu-Li J, Yao Z*, et al.* Global mapping of H3K4me3 and H3K27me3 reveals specificity and plasticity in lineage fate determination of differentiating CD4+ T cells. *Immunity* 2009, **30**(1)**:** 155-167.

25. Huang da W, Sherman BT, Lempicki RA. Systematic and integrative analysis of large gene lists using DAVID bioinformatics resources. *Nat Protoc* 2009, **4**(1)**:** 44-57.